Original Article
J Vet Sci 2015, 16(4), 397-404 · http://dx.doi.org/10.4142/jvs.2015.16.4.397

Effect of serum-derived albumin scaffold and canine adipose tissue-derived mesenchymal stem cells on osteogenesis in canine segmental bone defect model

Daeyoung Yoon[1], Byung-Jae Kang[2], Yongsun Kim[1,3], Seung Hoon Lee[1,3], Daeun Rhew[1], Wan Hee Kim[1], Oh-Kyeong Kweon[1,3,*]

[1]*Department of Veterinary Surgery, College of Veterinary Medicine, and* [3]*BK21 PLUS Program for Creative Veterinary Science Research, Research Institute for Veterinary Science and College of Veterinary Medicine, Seoul National University, Seoul 08826, Korea*
[2]*Department of Veterinary Surgery, College of Veterinary Medicine, Kangwon National University, Chuncheon 24341, Korea*

Composite biological and synthetic grafts with progenitor cells offer an alternative approach to auto- or allografts for fracture repair. This study was conducted to evaluate osteogenesis of autologous serum-derived albumin (ASA) scaffolds seeded with canine adipose tissue-derived mesenchymal stem cells (Ad-MSCs) in a canine segmental bone defect model. ASA scaffold was prepared with canine serum using cross-linking and freeze-drying procedures. Beta-tricalcium phosphate (β-TCP) was mixed at the cross-linking stage. Ad-MSCs were seeded into the scaffold and incubated for one day before implantation. After 16 weeks, the grafts were harvested for histological analysis. The dogs were divided into five groups: control, ASA scaffolds with and without Ad-MSCs, and ASA scaffolds including β-TCP with and without Ad-MSCs. ASA scaffolds with Ad-MSCs had a significantly larger area of increased opacity at the proximal and distal host cortex-implant interfaces in radiographs 16 weeks after implantation compared to the groups with β-TCP ($p < 0.05$). Histomorphometric analysis showed that ASA scaffolds with Ad-MSCs had significantly greater new bone formation than other groups ($p < 0.05$). These results suggest that Ad-MSCs seeded into ASA scaffolds enhanced osteogenesis in the bone defect model, but that β-TCP in the ASA scaffold might prevent penetration of the cells required for bone healing.

Keywords: adipose tissue-derived mesenchymal stem cells, bone defect, serum-derived albumin scaffold

Introduction

Repair of large segmental defects in the diaphyseal bone poses a daunting challenge to veterinarians. The classical standard of treatment uses autologous bone grafts or allografts [7], which are associated with substantial morbidity, including infection, disease transmission, and loss of function [1,8,12,14]. The complications resulting from graft harvest and the limited supply of grafts have necessitated the development of alternative strategies for the repair of clinically challenging bone defects. The primary approach to this problem has focused on the development of biological or synthetic implant materials and use of mesenchymal stem cells (MSCs) [7]. MSCs are multipotent cells derived from the bone marrow, adipose tissue, muscle, umbilical cord blood, and placenta that are capable of differentiating into myoblasts, tenocytes, chondrocytes, and adipocytes [7,24]. MSCs are also capable of differentiating along the osteoblastic lineage. We previously isolated and characterized MSCs derived from the adipose tissues of dogs [25]. Canine adipose tissue-derived MSCs (Ad-MSCs) are capable of differentiating into osteoblasts, and their advantages include easy and reproducible access to subcutaneous adipose tissue, simple isolation protocols, abundant supply, and a relatively noninvasive harvesting procedure [30].

Synthetic bone substitutes and materials with osteogenic potential have been evaluated as scaffold materials for the treatment of bone defects [2,31]. Among the synthetic bone substitutes, beta tricalcium phosphate (β-TCP) ceramics have shown the most promising results because of their osteoconductive properties, unlimited availability, and the absence of immune response [23,29]. Moreover, Ad-MSCs mixed with β-TCP have demonstrated osteogenic potential in

Received 3 Nov. 2014, Revised 8 May. 2015, Accepted 2 Jun. 2015
*Corresponding author: Tel: +82-2-880-1248; Fax: +82-2-888-2866; E-mail: ohkweon@snu.ac.kr
pISSN 1229-845X
eISSN 1976-555X

ectopic implantation [5].

In bone tissue engineering, appropriate scaffolds are essential to support cell growth and control osteogenic differentiation. For cell scaffolding, ideal scaffolds are highly porous materials with good biocompatibility and osteointegrative properties [15,26]. Serum-derived scaffolds possess great scaffolding potential due to their biologically porous structure and high seeding efficiency [11]. We previously showed that collagen I gel enhances osteogenic differentiation and homogenous distribution of Ad-MSCs seeded onto an autologous serum-derived albumin (ASA) scaffold [18]. In this study, we evaluated the osteogenic potential of canine ASA scaffold mixed with or without β-TCP and seeded with or without Ad-MSCs in a canine bone defect model.

Materials and Methods

ASA scaffolds

ASA scaffolds were fabricated according to the freeze-drying and chemical cross-linking procedures [10,11]. Briefly, 10 mL of canine blood was withdrawn by venipuncture and kept at 37°C for 30 min for fibrin clot retraction. The blood sample was then centrifuged at 1,260 × g for 15 min to obtain the serum, after which 0.5 mL of 25% glutaraldehyde solution (Sigma-Aldrich, USA) was added to 5 mL of the serum obtained for cross-linking. This serum was transferred to a 1 mL disposable syringe and kept until solidification. The solution was subsequently moved to a freezer and maintained at −70°C overnight. After cutting the syringe, the cross-linked frozen solution was lyophilized for 48 h in a freeze dryer (DFU-8603; Operon, Korea). Next, the cylindrical sponge-shaped, freeze-dried serum was obtained and rehydrated in graded ethanol series (100%, 90%, and 80%) by dipping in each concentration for 1 h. The obtained scaffold was then cut into 20 mm long columns and sterilized in 70% ethanol for 8 h. Next, the scaffold was neutralized in serum-free Dulbecco's Modified Eagle's Medium (DMEM; Gibco, USA), after which excess fluid was removed and the column-shaped scaffolds were placed in a 6-well plate (Thermo Scientific, USA) at one scaffold per well.

In this study, there were four experimental groups depending on the presence or absence of β-TCP and with or without the seeding of Ad-MSCs (panel A in Fig. 1). In groups with β-TCP, 5 mL of serum was added and simultaneously mixed with 0.5 mL of 25% glutaraldehyde solution and 300 mg β-TCP. This solution was then transferred to a 1 mL disposable syringe and rolled until solidification, after which it was processed as described above.

Preparation of β-TCP

β-TCP granules with particle sizes of 200 to 300 μm were kindly provided by the Biomaterial Center, National Institute for Material Science, Tsukuba, Japan [21].

Preparation of canine Ad-MSCs

Canine Ad-MSCs were obtained by culturing to facilitate the proliferation of mononucleated cells from adipose tissues as previously described [19,20]. Briefly, adipose tissues were aseptically collected from the gluteal region of a 2 year old beagle under general anesthesia. The adipose tissues were extensively washed with phosphate buffered saline (PBS), then minced with scissors, after which they were digested with 1 mg/mL collagenase type I (Sigma-Aldrich) for 2 h at 37°C. Next, the tissue samples were washed with PBS and centrifuged at 200 × g for 10 min. The resulting pellet containing the stromal vascular fraction was resuspended, filtered through a 100 μm nylon mesh, and then incubated overnight in DMEM with 10% fetal bovine serum (FBS; Gibco) at 37°C in a 5% CO_2 humidified atmosphere. After 24 h, unattached cells and residual non-adherent red blood cells were removed by washing

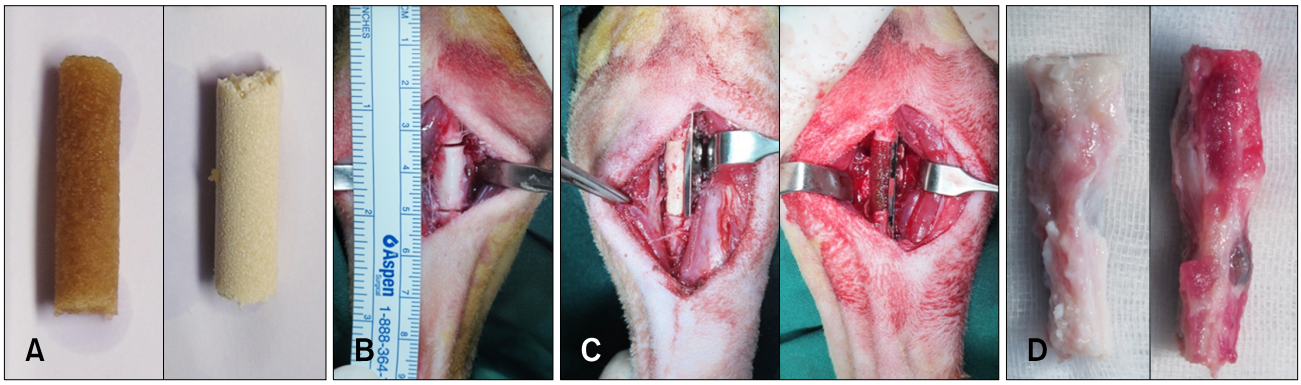

Fig. 1. The orthotopic implantation procedure. (A) Scaffold preparation: Left, autologous serum-derived albumin (ASA) scaffold; Right, ASA scaffold mixed with β-tricalcium phosphate (β-TCP). (B) Segmental defect in the ulnar diaphysis. (C) Filling the bone defect with the scaffold; Left, ASA scaffold mixed with β-TCP; Right, ASA scaffold. (D) Implant harvested after 16 weeks.

with PBS. The medium was replaced every 48 h until the cells became confluent. At 90% confluence, the cells were subcultured, and cells at passage 3 were used for seeding into the scaffolds.

Cell seeding

A suspension of 1×10^6 cells in 50 μL PBS was mixed with 250 μL purified bovine collagen solution (Nutragen; Advanced BioMatrix, USA) to improve the cell-adherent properties of the scaffolds and increase the rate of MSC-mediated bone formation [18]. The cells were seeded into the scaffolds placed in the wells of a 6-well plate and incubated in growth medium (DMEM supplemented with 10% FBS) at 37°C and 5% CO_2 for one day before *in vivo* implantation.

Orthotopic implantation and harvest

All animal procedures were performed in accordance with the guidelines of the Institutional Animal Care and Use Committee of Seoul National University (SNU-121217-1). Ten skeletally mature beagles (average weight of 8.95 ± 0.96 kg and average age of 1.3 ± 0.5 years) were used for the orthotopic implantation. The segmental resection of a portion of the ulna was performed bilaterally as previously described [22]. Briefly, dogs were sedated with an intravenous injection of acepromazine maleate (Sedaject; Samwoo Medical, Korea) at a dose of 0.01 mg/kg body weight and then premedicated with a subcutaneous injection of atropine sulfate (Jeil Pharmaceutical, Korea) at a dose of 0.1 mg/kg of body weight. Anesthesia was then induced by intravenous administration of a mixture of zolazepam/tiletamine (25 mg/mL, Zoletil 50; Virbac, France) at a dose of 5 mg/kg body weight and maintained with isoflurane (Aerane; Baxter, USA) in oxygen. Intravenously administered tramadol (Toranzin; Samsung Pharm, Korea) and cefazolin sodium (cefazolin injection; Chong Kun Dang, Korea) at a dose of 4 mg/kg and 22 mg/kg body weight were used as an analgesic and antibiotic, respectively. An anesthesia monitor (Datex-Ohmeda S/5; GE Healthcare, Finland) was used to monitor physiological factors including rectal temperature, oxygen saturation, end tidal CO_2, electrocardiogram, minimum alveolar concentration value, and pulse rate. The diaphysis of the ulna was exposed under sterile conditions using the caudal approach, after which the overlying periosteum was resected from the defect area. An eight hole, 2.7 dynamic compression plate (Synthes, Switzerland) was then contoured and applied to the medial portion of the ulna. The plate was subsequently removed, after which a 15 mm long osteoperiosteal segmental cortical defect was created at the mid-portion of the diaphysis with an oscillating saw (Stryker, USA) (panel B in Fig. 1). The defect was then filled with ASA scaffold (albumin [Alb], n = 4), ASA scaffold seeded with Ad-MSCs (Alb + Ad-MSCs, n = 4), albumin mixed with β-TCP scaffold (Alb + β-TCP, n = 4), albumin mixed with β-TCP scaffold plus Ad-MSCs (Alb + β-TCP + Ad-MSCs, n = 4), or nothing (control, n = 4) (panel C in Fig. 1). Next, the plate was reapplied, and the prepared scaffolds were implanted into the defect. Each dog received an implant at random on each ulna. After closing the soft tissue, a Robert Jones bandage was applied for 2 weeks. Two weeks after the surgery, all animals were active and fully capable of walking and bearing weight. The implants were harvested 16 weeks after implantation and used for histological examination (panel D in Fig. 1).

Radiographic examination

Lateral and craniocaudal radiographs of the antebrachium were made before and immediately after surgery, as well as 4, 8, and 16 weeks after implantation. All radiographs assessed the total area of new bone formation at the proximal and distal host cortex-implant interfaces. Radiographic imaging software (Infinitt Pacs; INFINITT Healthcare, Korea) was used to measure the area occupied by the newly formed bone.

Histological examination

A 5 cm segment of the bone including the defect site was harvested and fixed in 4% paraformaldehyde. The samples were then decalcified with hydrochloric acid, dehydrated in a series of ethanol solutions, and longitudinally embedded in paraffin. Next, samples were cut in the sagittal plane. The central longitudinal sections from each ulna were subsequently placed on the ground and cut to a thickness of 100 μm, after which they were stained with H&E and Massons's trichrome stain to evaluate new bone formation.

The stained sections from each group were observed under a light microscope and scanned using an attached digital camera and a NIS-Elements system (Nikon, Japan). For histomorphometric analysis, all groups were analyzed according to the following protocol. The entire implant area was viewed in six microscopic fields, and each field was captured using a digital camera and then subjected to histomorphometric analyses. The interface between the new bone and host bone in the histological picture was marked by measuring the distance from the screw hole in the radiographs. The newly formed bone area was estimated and converted into a percentage of the total implanted area using image processing and analysis software (ImageJ 1.49; National Institute of Health, USA).

Statistical analysis

Data were analyzed using the SPSS statistical analysis software (ver. 18.0; SPSS, USA). The Kruskal-Wallis test was used to assess differences among groups. A post-hoc test was performed along with a Mann-Whitney U test. A p value < 0.05 was considered to indicate statistical significance.

Results

Radiographic findings

In all groups, reactive bone formation at the transversely cut edges of the host ulna was observed at 4 weeks. By 16 weeks, slightly increased bone formation was visible within the gap, especially along the scaffold in all groups except the control. In the control group, similar changes such as reactive bone formation were limited to areas near the interface with the host bone (panel A in Fig. 2). The implanted sites in groups containing β-TCP could be easily visualized because of the radiopacity of the β-TCP particles (panels D and E in Fig. 2).

Radiomorphometric analysis showed that all of the treated groups had significantly larger areas of increased opacity at the proximal and distal host cortex-implant interfaces compared to the control group ($p < 0.05$). In addition, the groups with β-TCP showed a smaller area of increased opacity at the proximal and distal host cortex-implant interfaces compared to the Alb + Ad-MSCs groups ($p < 0.05$) (Table 1).

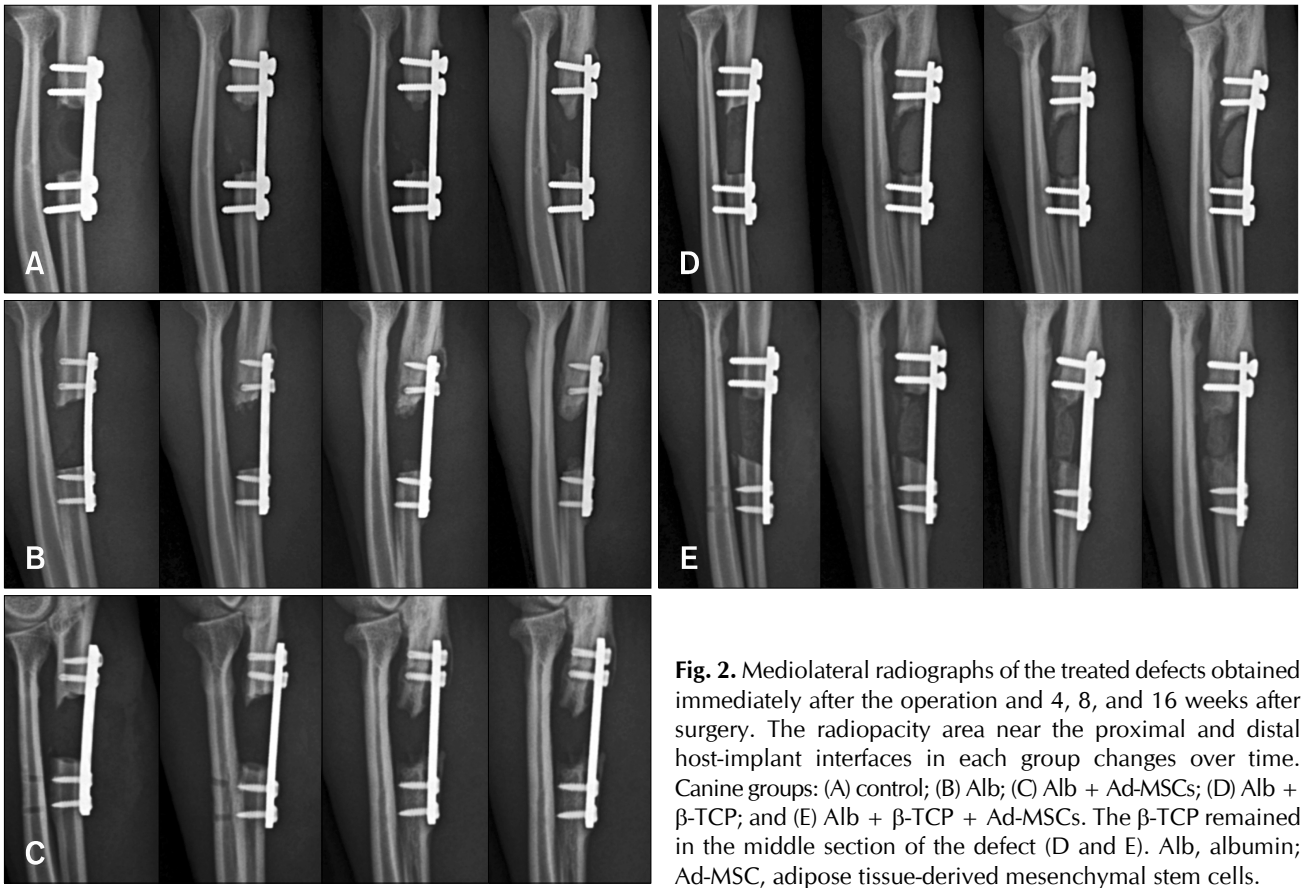

Fig. 2. Mediolateral radiographs of the treated defects obtained immediately after the operation and 4, 8, and 16 weeks after surgery. The radiopacity area near the proximal and distal host-implant interfaces in each group changes over time. Canine groups: (A) control; (B) Alb; (C) Alb + Ad-MSCs; (D) Alb + β-TCP; and (E) Alb + β-TCP + Ad-MSCs. The β-TCP remained in the middle section of the defect (D and E). Alb, albumin; Ad-MSC, adipose tissue-derived mesenchymal stem cells.

Table 1. Radiomorphometric analysis of the total area (in mm^2) of new bone formation at the proximal and distal host cortex-implant interfaces at 4, 8, and 16 weeks after implantation

Groups	4 weeks after implantation	8 weeks after implantation	16 weeks after implantation
Control	4.90 ± 2.23	5.57 ± 2.25	6.48 ± 2.40
Alb	4.16 ± 2.04	10.08 ± 4.86	15.33 ±5.21*
Alb + Ad-MSCs	5.47 ± 2.62	10.64 ± 3.63	19.43 ± 3.45*
Alb + β-TCP	3.57 ± 2.30	5.84 ± 2.40	10.29 ± 3.37*,†
Alb + β-TCP + Ad-MSCs	4.60 ± 2.17	6.63 ± 2.50	11.51 ± 3.62*,†

Data are presented as the means ± SD. *Significant difference ($p < 0.05$) compared to the control. †Significant difference ($p < 0.05$) compared to the Alb + Ad-MSCs group.

Histological findings

In all experimental groups, new bone formation was observed in longitudinal sections throughout the segmental bone defect at 16 weeks after implantation. Histologically, no adverse host response was detected and newly formed bone was primarily observed at the cortex-implant interfaces, especially the proximal portion. Some of the areas in the middle section of the bone defect were filled with fibrous connective tissue (Fig. 3). In the β-TCP-applied group, the β-TCP remained in the middle section of the defect (Figs. 3 and 4). The Alb + Ad-MSCs group showed chondrocytic changes and new woven trabecular bone formation (Fig. 4).

The bone formation capacity was assessed from the histological images of all the groups by measuring the area of the newly formed bone (Fig. 3). The percentage of new bone formation out of the total area was significantly higher in all treated groups than the control group ($p < 0.05$) (Table 2). The histomorphometric analysis was consistent with the visual scoring, confirming that the Alb + Ad-MSCs group had a significantly larger area of bone formation than the Alb + β-TCP and Alb + β-TCP + Ad-MSCs groups ($p < 0.05$). Moreover, the Alb + Ad-MSCs group had significantly greater bone formation at the implant-to-host bone interfaces than the Alb group ($p < 0.05$) (Table 2).

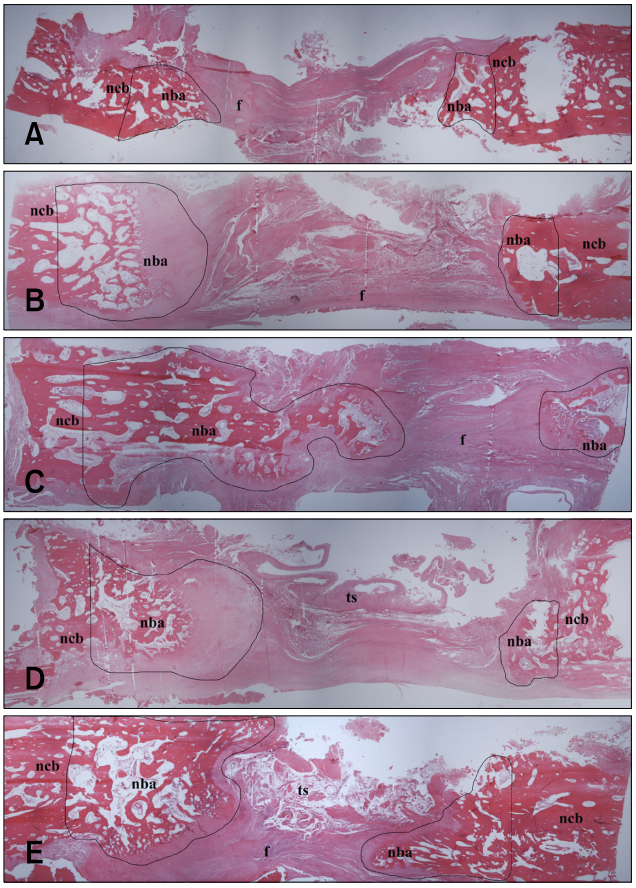

Fig. 3. Histological findings in longitudinal sections of the segmental bone defects 16 weeks after implantation. The merged picture of the entire defect area, including the adjacent normal bone areas in each group, is shown: (A) Control, (B) Alb, (C) Alb + Ad-MSCs, (D) Alb + β-TCP, and (E) Alb + β-TCP + Ad-MSCs. The proximal portion of the longitudinal section is shown in the left panels (A-E). All experimental groups showed increased bone formation compared to the control group. H&E stain. ncb, native cortical bone area; nba, newly formed bone area; f, fibrous tissue; ts, ASA scaffold mixed with β-TCP.

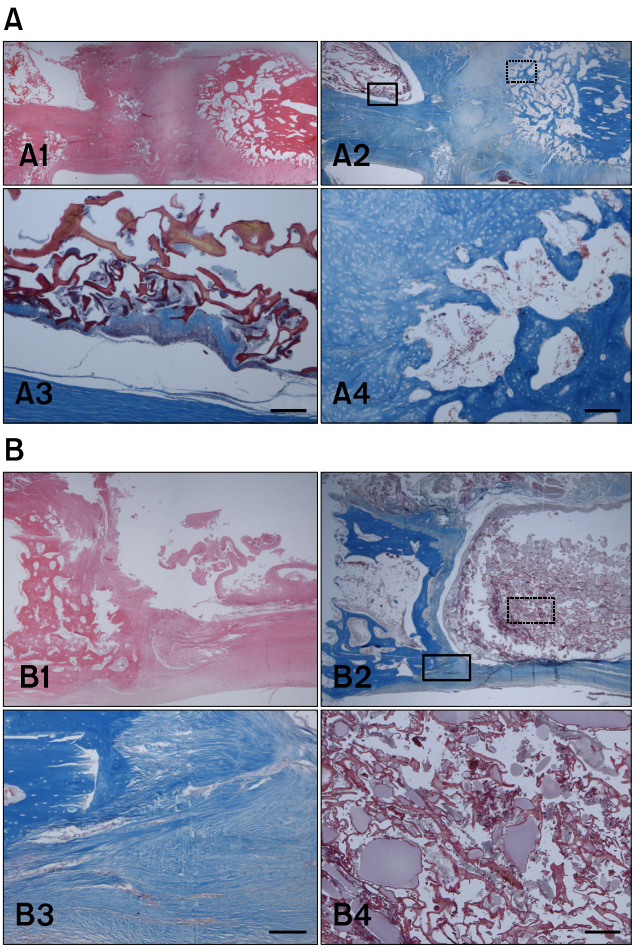

Fig. 4. Histological findings in the longitudinal sections of the interfacial area between bone defect and host bone 16 weeks after implantation. Canine groups (A) Alb + Ad-MSCs, (B) Alb + Ad-MSCs + β-TCP groups. (A2 and B2) Merged picture of the defect area including interfacial areas and implanted scaffold. (A3) The remaining ASA scaffold, solid frame of A2. (A4) Chondrocytic change and new woven bone formation, dot frame of A2. (B3) Fibrous tissue, solid frame of B2. (B4) The remaining ASA scaffold mixed with β-TCP, dot frame of B2. H&E staining (A1 and B1), Masson's trichrome staining (A2-4 and B2-4). Magnification: 100× (A3 and 4), 40× (B3 and 4). Scale bars = 200 μm (A3 and 4), 400 μm (B3 and 4).

Table 2. Histomorphometric analysis of new bone formation at the proximal and distal host cortex-implant interfaces at 16 weeks after implantation

Groups	NBA/TA (%)
Control	13.30 ± 3.11†
Alb	29.78 ± 3.98*,†
Alb + Ad-MSCs	36.07 ± 5.72*
Alb + TCP	22.83 ± 3.21*,†
Alb + TCP + Ad-MSCs	23.37 ± 4.54*,†

Data are presented as the means ± SD. *Indicates a statistically significant difference ($p < 0.05$) compared to the control. †Indicates a statistically significant difference ($p < 0.05$) compared to the Alb + Ad-MSCs group. NBA, newly formed bone area TA, total implanted area.

Discussion

The objective of this study was to evaluate the effect of Ad-MSCs, β-TCP, and ASA scaffold on bone regeneration in canine segmental bone defects. Previous studies [10,11] have confirmed the clinical feasibility of ASA loaded with alveolar cells as a promising alternative for bone regeneration. ASA scaffold with collagen I gel provides a favorable biological and mechanical environment for osteogenic differentiation of MSCs [18]. Our results demonstrate that the combination of an Ad-MSCs and ASA scaffold can support osteogenesis for the repair of segmental defects in the canine long bone.

The role of seeding cells in tissue regeneration is still controversial. Some groups have shown that the scaffold alone is sufficient for bone regeneration [6,32]. However, the results of this study demonstrate that groups without Ad-MSCs showed very little osseous tissue formation, which could be observed from the sawed edge of the surrounding normal bone. In minor bone defects, native cells with osteogenic potential are known to migrate into the scaffold to generate new osseous tissues and facilitate bone repair [5]. However, if the scaffold alone is implanted in critical-sized defects, either the migration rate or the amount of native cells from the surrounding tissue may not be fast enough or sufficient to efficiently produce bone tissue before degradation of the scaffold, resulting in the formation of scar tissue at the defect. Studies using bone marrow-derived MSCs (BM-MSCs) for bone regeneration have demonstrated that seeded BM-MSCs not only provide an osteogenic cell source for new bone formation, but also secrete growth factors to recruit native cells into the defect site [3,9,13]. In addition, significant levels of cytokines released by canine umbilical cord blood-derived MSCs one day after implantation can enhance bone regeneration [5]. Ad-MSCs may potentiate bone matrix deposits formed under osteogenic conditions and have an osteogenic differentiation capability [20]. We speculate that the acceleration of bone formation observed in the present study was induced by the growth factors secreted and the direct osteogenic differentiation facilitated by the Ad-MSCs.

The selection of an appropriate scaffold material for the Ad-MSCs used in bone repair remains a daunting challenge. The scaffolds serve as temporary matrices for bone regeneration and provide favorable conditions for cellular attachment, growth, and differentiation [7]. Scaffolds are three-dimensional, physical materials that offer an appropriate framework and surface characteristics for the adherence of MSCs, osteoblasts, osteocytes, chondroblasts, and chondrocytes [4,16]. In addition, scaffolds should be biocompatible to minimize interference from an inflammatory reaction during bone formation, biodegradable to match the expected rate of progressive bone replacement in the bone defect site, and provide mechanical support for osteogenesis [15,28]. MSCs combined with β-TCP show increased bone formation and osteogenic activity relative to those combined with any other clinically approved scaffold [27]. We previously verified the most effective concentration of β-TCP in ectopic implantation; however, this concentration may not be suitable for the ASA scaffold used in the present study. We found that the ASA scaffold with β-TCP displayed unfavorable resorption properties compared to the previous study [33]. Although the absorption of β-TCP was expected to positively influence bone formation [5], almost no new bone formation occurred within the implant site in the groups with β-TCP. These findings are considerably different from those of previous studies [17,20]. A porous scaffold microstructure with a minimal pore size of 100 to 150 μm is usually required to allow tissue ingrowth [34]. However, the mixed β-TCP appeared to fill the porous structure of the ASA scaffold, suggesting that it does not allow cellular penetration, extracellular matrix production, or neovascularization.

The histological findings confirmed that the ASA scaffold is biocompatible and does not induce any inflammatory reaction during the experimental period. This indicates that the ASA scaffold may also provide a favorable environment for osteogenic formation, similar to in vitro conditions [18]. In addition, some areas in the middle of the defect sites in the treatment groups were filled with fibrous connective tissue. Further research is necessary to investigate whether the fibrous tissue can be converted to osteogenic tissue. In conclusion, the results of the present study demonstrate that an ASA scaffold seeded with canine Ad-MSCs can accelerate new bone formation in canine segmental bone defects.

Acknowledgments

This work was supported partially by the Research Institute for Veterinary Science, Seoul National University, and the National Research Foundation of Korea (NRF-2013R1A 1A2004506).

Conflict of Interest

There is no conflict of interest.

References

1. **Aho AJ, Ekfors T, Dean PB, Aro HT, Ahonen A, Nikkanen V.** Incorporation and clinical results of large allografts of the extremities and pelvis. Clin Orthop Relat Res 1994, **307**, 200-213.
2. **Arinzeh TL, Tran T, Mcalary J, Daculsi G.** A comparative study of biphasic calcium phosphate ceramics for human mesenchymal stem-cell-induced bone formation. Biomaterials 2005, **26**, 3631-3638.
3. **Bi LX, Simmons DJ, Mainous E.** Expression of BMP-2 by rat bone marrow stromal cells in culture. Calcif Tissue Int 1999, **64**, 63-68.
4. **Bucholz RW.** Nonallograft osteoconductive bone graft substitutes. Clin Orthop Relat Res 2002, **395**, 44-52.
5. **Byeon YE, Ryu HH, Park SS, Koyama Y, Kikuchi M, Kim WH, Kang KS, Kweon OK.** Paracrine effect of canine allogenic umbilical cord blood-derived mesenchymal stromal cells mixed with β-tricalcium phosphate on bone regeneration in ectopic implantations. Cytotherapy 2010, **12**, 626-636.
6. **Clokie CML, Moghadam H, Jackson MT, Sandor GKB.** Closure of critical sized defects with allogenic and alloplastic bone substitutes. J Craniofac Surg 2002, **13**, 111-121.
7. **Drosse I, Volkmer E, Capanna R, De Biase P, Mutschler W, Schieker M.** Tissue engineering for bone defect healing: an update on a multi-component approach. Injury 2008, **39** (Suppl), S9-20.
8. **Ehrler DM, Vaccaro AR.** The use of allograft bone in lumbar spine surgery. Clin Orthop Relat Res 2000, **371**, 38-45.
9. **Frank O, Heim M, Jakob M, Barbero A, Schäfer D, Bendik I, Dick W, Heberer M, Martin I.** Real-time quantitative RT-PCR analysis of human bone marrow stromal cells during osteogenic differentiation in vitro. J Cell Biochem 2002, **85**, 737-746.
10. **Gallego L, Junquera L, García E, García V, Álvarez-Viejo M, Costilla S, Fresno MF, Meana Á.** Repair of rat mandibular bone defects by alveolar osteoblasts in a novel plasma-derived albumin scaffold. Tissue Eng Part A 2010, **16**, 1179-1187.
11. **Gallego L, Junquera L, Meana Á, Álvarez-Viejo M, Fresno M.** Ectopic bone formation from mandibular osteoblasts cultured in a novel human serum-derived albumin scaffold. J Biomater Appl 2010, **25**, 367-381.
12. **Garbuz DS, Masri BA, Czitrom AA.** Biology of allografting. Orthop Clin North Am 1998, **29**, 199-204.
13. **Harris SE, Sabatini M, Harris MA, Feng JQ, Wozney J, Mundy GR.** Expression of bone morphogenetic protein messenger RNA in prolonged cultures of fetal rat calvarial cells. J Bone Miner Res 1994, **9**, 389-394.
14. **Head WC, Emerson RH Jr, Malinin TI.** Structural bone grafting for femoral reconstruction. Clin Orthop Relat Res 1999, **369**, 223-229.
15. **Hutmacher DW.** Scaffolds in tissue engineering bone and cartilage. Biomaterials 2000, **21**, 2529-2543.
16. **Ishaug SL, Crane GM, Miller MJ, Yasko AW, Yaszemski MJ, Mikos AG.** Bone formation by three-dimensional stromal osteoblast culture in biodegradable polymer scaffolds. J Biomed Mater Res 1997, **36**, 17-28.
17. **Jang BJ, Byeon YE, Lim JH, Ryu HH, Kim WH, Koyama Y, Kikuchi M, Kang KS, Kweon OK.** Implantation of canine umbilical cord blood-derived mesenchymal stem cells mixed with beta-tricalcium phosphate enhances osteogenesis in bone defect model dogs. J Vet Sci 2008, **9**, 387-393.
18. **Kang BJ, Kim Y, Lee SH, Kim WH, Woo HM, Kweon OK.** Collagen I gel promotes homogenous osteogenic differentiation of adipose tissue-derived mesenchymal stem cells in serum-derived albumin scaffold. J Biomater Sci Polym Ed 2013, **24**, 1233-1243.
19. **Kang BJ, Ryu HH, Park SS, Kim Y, Woo HM, Kim WH, Kweon OK.** Effect of matrigel on the osteogenic potential of canine adipose tissue-derived mesenchymal stem cells. J Vet Med Sci 2012, **74**, 827-836.
20. **Kang BJ, Ryu HH, Park SS, Koyama Y, Kikuchi M, Woo HM, Kim WH, Kweon OK.** Comparing the osteogenic potential of canine mesenchymal stem cells derived from adipose tissues, bone marrow, umbilical cord blood, and Wharton's jelly for treating bone defects. J Vet Sci 2012, **13**, 299-310.
21. **Kikuchi M, Koyama Y, Yamada T, Imamura Y, Okada T, Shirahama N, Akita K, Takakuda K, Tanaka J.** Development of guided bone regeneration membrane composed of β-tricalcium phosphate and poly ($_{L}$-lactide-*co*-glycolide-*co*-ε-caprolactone) composites. Biomaterials 2004, **25**, 5979-5986.
22. **Nilsson OS, Urist MR, Dawson EG, Schmalzried TP, Finerman GAM.** Bone repair induced by bone morphogenetic protein in ulnar defects in dogs. J Bone Joint Surg Br 1986, **68**, 635-642.
23. **Oonishi H.** Orthopaedic applications of hydroxyapatite. Biomaterials 1991, **12**, 171-178.
24. **Pittenger MF, Mackay AM, Beck SC, Jaiswal RK, Douglas R, Mosca JD, Moorman MA, Simonetti DW, Craig S, Marshak DR.** Multilineage potential of adult human mesenchymal stem cells. Science 1999, **284**, 143-147.
25. **Ryu HH, Lim JH, Byeon YE, Park JR, Seo MS, Lee YW, Kim WH, Kang KS, Kweon OK.** Functional recovery and neural differentiation after transplantation of allogenic adipose-derived stem cells in a canine model of acute spinal cord injury. J Vet Sci 2009, **10**, 273-284.
26. **Salgado AJ, Coutinho OP, Reis RL.** Bone tissue engineering: state of the art and future trends. Macromol Biosci 2004, **4**, 743-765.
27. **Sanchez-Sotelo J, Munuera L, Madero R.** Treatment of fractures of the distal radius with a remodellable bone cement: a prospective, randomised study using Norian SRS. J Bone Joint Surg Br 2000, **82**, 856-863.
28. **Sandhu HS, Grewal HS, Parvataneni H.** Bone grafting for spinal fusion. Orthop Clin North Am 1999, **30**, 685-698.
29. **Sartoris DJ, Holmes RE, Resnick D.** Coralline hydroxyapatite bone graft substitutes: radiographic

evaluation. J Foot Surg 1992, **31**, 301-313.
30. **Schäffler A, Büchler C.** Concise review: adipose tissue-derived stromal cells—basic and clinical implications for novel cell-based therapies. Stem cells 2007, **25**, 818-827.
31. **Tseng SS, Lee MA, Reddi AH.** Nonunions and the potential of stem cells in fracture-healing. J Bone Joint Surg Am 2008, **90** (Suppl 1), 92-98.
32. **Ueki K, Takazakura D, Marukawa K, Shimada M, Nakagawa K, Takatsuka S, Yamamoto E.** The use of polylactic acid/polyglycolic acid copolymer and gelatin sponge complex containing human recombinant bone morphogenetic protein-2 following condylectomy in rabbits. J Craniomaxillofac Surg 2003, **31**, 107-114.
33. **van Hemert WLW, Willems K, Anderson PG, van Heerwaarden RJ, Wymenga AB.** Tricalcium phosphate granules or rigid wedge preforms in open wedge high tibial osteotomy: a radiological study with a new evaluation system. Knee 2004, **11**, 451-456.
34. **Zeltinger J, Sherwood JK, Graham DA, Müeller R, Griffith LG.** Effect of pore size and void fraction on cellular adhesion, proliferation, and matrix deposition. Tissue Eng 2001, **7**, 557-572.